Available online at **www.joac.info**

ISSN: 2278-1862

Journal of Applicable Chemistry

2013, 2 (1): 66-72

(International Peer Reviewed Journal)

Sonolytic Decolourisation of Acid Red 88 Dye in the presence of Titanium Dioxide and some Rare Earths

Pankaj Srivastava*, Prem Kishore Patnala, Shikha Goyal

*Department of Chemistry, Dayalbagh Educational; Institute, Agra 282 005, INDIA

Email: pankaj2@bsnl.in

Received on 18th December and finalized on 28th December 2012

ABSTRACT

The decolourisation of Acid Red 88 (AR-88), in the presence of ultrasound (US), TiO_2 and rare earth (REs) ions (La^{+3}, Pr^{+3}, Gd^{+3}, Ce^{+3}) in the aqueous solution, has been examined in the dye concentration range from 24 –48 ppm. AR-88 was decolorized to about 97.19% in the presence of US+TiO_2+Gd in 40 min. The rate of decolourisation was estimated spectrophotometrically from the residual concentration of dye and found to decrease in the order, in systems comprising; US+TiO_2+Gd > US+TiO_2+La > US+TiO_2+Ce > US+TiO_2+Pr > US+TiO_2 > US+Gd > US+La > US+Ce > US+Pr >TiO_2>US. Adsorption behaviour has been analysed using Langmuir, Freundlich and Temkin adsorption isotherms. It was found that adsorption followed pseudo second order kinetics. The mechanism of dye adsorption process was determined from the Weber-Morris intraparticle diffusion and Boyd kinetic models. The decolourisation of dye was maximum in the presence of rare earths due to the enhancement of adsorption of dye on RE-TiO_2 as a result of a chemical complexation between RE and the dye, through the donation of non-bonding electron pair from the elements of dye to the vacant f-orbitals of RE and the subsequent transfer of the complex to the TiO_2 surface. In the presence of rare earth cations, the surface of TiO_2 particles, which was negatively charged, is mostly occupied with positively charged rare earth ions. Thus the adsorption of AR-88 was enhanced on the surface of TiO_2 through electrostatic attraction, resulting into sand witched structure between TiO_2, REs and Dye molecule. A detailed sonochemical degradation pathway has been suggested based on electro spray ionization mass spectrometry (ESI-MS).

Keywords: Ultrasound, Adsorption, Kinetics, TiO_2, Rare Earths.

INTRODUCTION

In continuation with our work on the sonochemical adsorption and degradation of dyes on TiO_2 in the presence of rare earth ions (REs) [1-4], we hereby report the adsorption and degradation study of Acid Red 88 (AR88) due to ultrasound (20 kHz, 250 W) and rare earths (La, Pr, Gd & Ce). The decolourisation effects of ultrasound results from acoustic cavitation, which includes the formation, growth and impulsive collapse of bubbles in liquid [5-8]. Dissolved gases in the water act as the first site of nucleation for cavitating bubbles [9-10]. The sudden collapse of bubbles cause high local temperature (>4000K) and pressure (>1000atm) resulting into a homogenous splitting of water into $^{\bullet}OH$ and $^{\bullet}H$ radicals. In the first step the rare earths facilitate complex formation with dye molecules, whereas in the following step the

ultrasound promotes transfer and adsorption of these complexes onto the surface of TiO_2. The nature of adsorption has been examined through Langmuir [11], Freundlich [12] and Temkin [13] adsorption isotherms, whereas, the mechanism has been investigated through Weber–Morris [14] and Boyd [15] models.

MATERIALS AND METHODS

AR-88 [99.9% purity] was received as gift from M/s Spectrum Dyes and Chemicals, Surat, India and its structure is given in Fig.1. Lanthanum chloride, Gadolinium chloride, Praseodymium chloride and Cerium chloride [Indian Rare Earths Ltd, 99.99%] were kept under vacuum for 2hr before use. Titanium (IV) isopropoxide (Sigma Aldrich [> 97 % purity] was used without further purification.

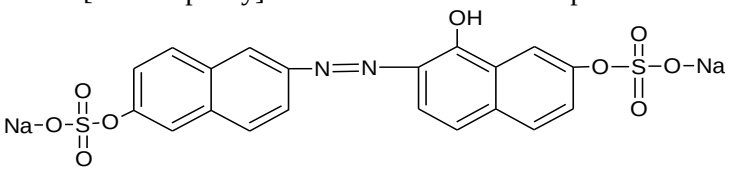

Fig. 1 Structure of Acid Red 88

A stock solution (1000 mg L^{-1}) of AR 88 was prepared in triple distilled deionised water. In 10 mL of dye solution at different concentration from 24-48 mg L^{-1}, 0.02 mL of Titanium (IV) isopropoxide (184 mg L^{-1} of TiO_2) and 5mL of 20 mg L^{-1} RE^{3+} ions were added and the solution was sonicated for 8 to 40 minutes using Vibronics Processor, operating at 20 kHz and 250W. The sorption of AR 88 was then carried out on TiO_2 in the presence or absence of ultrasound, TiO_2 & REs. The test solutions were filtered through Whatman filter paper 3 and the concentration of the residual amount of AR88 was determined on Shimadzu UV-Visible spectrophotometer, 1601 PC at λ_{max} =507nm.The amount of Acid Red 88 adsorbed onto Titanium Isopropoxide (IV) was calculated by using the following expression [16]:

$$q_t = [(C_o - C_t)x\ V]/M \quad (1)$$

where C_o is the initial concentration of dye and C_t is the concentration of dye at time t, V is the volume of solution (L) and M is the mass of adsorbent (g).

The sonochemical degradation pathway of AR 88 was studied using electro spray ionization mass spectra (ESI-MS), performed on a Water Q- TOF micro Y A-260 (Micro mass) tandem quadruple orthogonal TOF instrument, fitted with a lock spray source. The analysis was carried out with capillary voltage of 2220 V, sample cone of 30 V, source temperature of 110ºC and syringe rate of 10µl respectively.

RESULTS AND DISCUSSION

Adsorption Isotherms : Adsorption isotherms are mathematical models that describe the distribution of the adsorbate species among liquid and adsorbent, based on a set of assumptions that are mainly related to the heterogeneity/homogeneity of adsorbents, the type of coverage and possibility of interaction between the adsorbate species.

In this work, the models of Langmuir [11], Freundlich [12], and Temkin [13] were used to describe the relationship between the amount of dye adsorbed, q_e and its equilibrium concentration C_e. The linear forms of the above mentioned adsorption isotherms are expressed by equations (2-4) respectively.

$$C_{eq}/q_e = 1/q_m b + C_{eq}/q_m \quad (2)$$

$$\log q_e = \log K_F + n \log C_{eq} \quad (3)$$

$$q_e = a + b \log C_{eq} \quad (4)$$

Langmuir isotherm constants, q_m and b as shown in Table.1, related to the theoretical maximum adsorption capacity (mg g^{-1}) and the energy of adsorption ($dm^{-3}g^{-1}$) respectively. The essential characteristics of Langmuir equation were expressed in terms of dimensionless separation factor R_L [17] and its calculated

value between 0 and 1 (Table.1) indicates the favourable adsorption of dye. K_F and n are the Freundlich constants as shown in Table.1, representing the adsorption capacity ($dm^{-3}g^{-1}$) and adsorption intensity respectively. Value of n between 1 to10 (Table.1) indicates an effective adsorption. a and b are the Temkin isotherm constants, where a represents the equilibrium binding constants and b is the intensity of adsorption and its calculated values are shown in Table.1.

Table.1 Isotherm parameters for the adsorption of AR 88 dye at different experimental conditions.

Experimental conditions	Langmuir			Freundlich			Temkin		
	q_m (mg/g)	R_L	R^2	K_F (mg/g)	n (Lmg^{-1})	R^2	a (mg/g)	b (Lmg^{-1})	R^2
US+TiO_2	116.19	0.09	0.97	1.116	7.8659	0.98	3.23	303.68	0.99
TiO_2	85.418	0.08	0.99	13.591	0.2168	0.98	2.69	29.055	0.95
US+TiO_2+Pr	224.73	0.17	0.99	110.77	1.3964	0.98	105.41	525.09	0.99
TiO_2+Pr	187.76	0.23	0.94	98.74	0.9430	0.95	92.35	323.43	0.92
US+TiO_2 + Ce	226.25	0.09	0.99	106.78	0.7956	0.98	106.78	310.24	0.99
TiO_2 + Ce	212.28	0.04	0.98	100.92	0.2088	0.97	95.67	78.905	0.95
US+ TiO_2+ La	233.52	0.06	0.99	120.02	0.7697	0.95	120.02	303.63	0.98
TiO_2 + La	214.05	0.15	0.97	101.15	0.8985	0.97	96.36	323.39	0.95
US+ TiO_2+ Gd	257.89	0.27	0.99	106.45	0.3526	0.98	106.45	130.33	0.99
TiO_2+ Gd	218.61	0.08	0.99	104.49	0.5843	0.99	104.49	227.18	0.95

Adsorption kinetics: The kinetics [18] of adsorption of dye on the TiO_2 surface has been found to pursue pseudo second order, and is expressed as

$$t/q_t = 1/h + t/q_e \quad (5)$$

where, q_e is the amount of dye adsorbed at equilibrium (mg/g), q_t is the amount of dye adsorbed at time t (mg/g), $h= kq_e^2$; k is the second order adsorption rate constant (g $mg^{-1}min^{-1}$). The q_e values shown in Table.2 were obtained from the slope and intercept of linear plot of t/q_t versus t.

Table.2 Pseudo Second Order Data of Acid Red 88

Experimental conditions	Pseudo second order	
	q_e(cal.) mg/g	R^2
US+TiO_2	10.408	0.99
TiO_2	9.57	0.99
US+TiO_2+Pr	92.02	0.99
TiO_2+Pr	84.03	0.99
US+TiO_2+Ce	96.89	0.99
TiO_2+Ce	89.05	0.99
US+TiO_2+La	98.58	0.99
TiO_2+La	91.74	0.99
US+TiO_2+Gd	107.87	0.99
TiO_2+Gd	106.15	0.99

Adsorption Mechanism: A mechanism of adsorption of AR 88 dye can now be explained as under;
Maximum decolourisation of the dye, AR88, was in the presence of rare earths. Thus REs facilitate adsorption, first by making a complex with the AR88 molecules, as indicated through a shift in λ_{max} from 510 to 507 nm and then transporting them towards the electro(-)vely charged surface of the TiO_2.The chemical complexation between REs and the dye molecule occurs through the donation of non-bonding electron pair from the donor elements of dye to the vacant *f*-orbitals of REs. In the presence of rare earth cations, the surface of TiO_2 particles, which was negatively charged, is mostly occupied with positively charged rare earth ions. Thus the adsorption of AR-88 was enhanced on the surface of TiO_2 through electrostatic attraction, resulting into a sand witched structure between TiO_2, REs and Dye molecule.
The mechanism of kinetic adsorption can now be confirmed by applying the experimental data to the Weber and Morris intra-particle diffusion and Boyd kinetic Models.
Weber Morris Kinetic model: The intraparticle diffusion model [14] is expressed by equation (6)

$$q_t = k_p t^{1/2} + c \quad (6)$$

q_t (mol.g^{-1}) is the amount of dye sorbed at time t, k_p is the intraparticle rate constant (g mg^{-1} min^{-1}) and c is the intercept obtained from the linear plot of q_t versus $t^{1/2}$ as shown in Table.3. Since the linear plot did not pass through the origin, the intraparticle diffusion was not the rate limiting step [14].
Boyd –Kinetic Model: Boyd kinetic model [15] is given by the equation (7)

$$Bt = -0.4977 - \ln(1 - F) \quad (7)$$

where $F = q_t/q_e$, represents the fraction of dye adsorbed at any time t, here q_e represents amount of dye adsorbed at equilibrium (mg/g) and q_t represents the amount of dye adsorbed at any time t(min) and B_t is a mathematical fraction of F.
The linear plot of B_t versus t can be employed to test whether sorption was controlled by film diffusion or particle diffusion. In our studies, the plots were linear but did not pass through the origin as predicted from intercept 'c' (Table.3) and therefore the adsorption process was controlled only by the film diffusion[15].

Table.3 Data showing Parameters of Weber-Morris and Boyd Kinetic Model

Experimental conditions	Weber and Morris Intraparticle diffusion model			Boyd Kinetic Model	
	K_p	c	R^2	c	R^2
US+TiO_2 TiO_2	1.24 0.99	61.64 12.35	0.95 0.94	2.05 0.15	0.89 0.92
US+ TiO_2+ Pr TiO_2+ Pr	4.08 0.72	110.25 97.97	0.96 0.96	2.13 3.16	0.97 0.97
US+ TiO_2+ Ce TiO_2+ Ce	3.24 2.94	109.92 97.48	0.98 0.99	3.20 2.13	0.94 0.98
US+ TiO_2+ La TiO_2+ La	0.55 3.34	108.30 100.97	0.88 0.99	3.43 2.79	0.89 0.99
US+TiO_2+Gd TiO_2+Gd	0.49 0.49	103.34 102.76	0.98 0.96	3.43 3.17	0.99 0.95

Sonochemical Degradation pathway of Acid Red 88 : To study the sonolytic degradation pathway of Acid Red 88 (AR 88) dye and identify the possible intermediate products, the sample was sonicated for 2 hr and examined immediately by Electrospray ionization mass spectrometer (ESI-MS) and Raman spectrometer. Major intermediates during the degradation process were proposed by using m/z values of the mass spectra. The ESMS analysis showed peaks at m/z values such as 106, 129, 138, 144, 152, 159, 175, 201, 223, 239, 255 and the possible structures matching the above mass values are presented in scheme 1. The degradation path is proposed to initiate through two different routes.

In the first path, sonochemical degradation of AR 88 involved the formation of new intermediate products with the addition of hydroxyl radical to an azo bond which give the product with m/z value 397, followed by cleavage of this bond to form hydroxyl amino naphthol (m/z = 175) and 4-aminonaphthalene sulphonic acid (m/z = 223). The hydroxyl radical attack of 4-aminonaphthalene sulphonic acid on different position form products with m/z values 239 and 255. The peak at m/z = 201 of 4-amino-2-formyl benzene sulphonic acid was also determined as an oxidation product of peak at 223.

The formation of hydroxylated products in first path is similar to previously reported literature on the degradation of AR 88 dye [19], besides the other probable intermediate products could also occur as shown in second path in scheme 1 of our study. The second path is proposed to start with the attack of $OH^{\cdot}$ radical which destroys the chromophoric system through azo bond cleavage and leads to the formation of possible intermediate i.e. amino naphthanol (m/z = 159). The dehydroxylation and deamination may provide the peak corresponding to m/z = 144 (aminonaphthalene) and m/z = 129 (naphthalene), respectively. Further degradation of 1,2-dimethyl benzene (m/z = 106), followed by subsequent oxidation leads to the formation of peaks corresponding to m/z values of 138 and 152, respectively.

The overlap density heatmap of the unsonicated and sonicated Raman spectra of AR 88 is shown in Fig. 2 by color coding. It could be seen that peaks in the sonicated and unsonicated solutions are different. Raman spectra of AR 88 recorded after sonicating the solution showed the shift in peaks in the region of 1600 to 1200 cm^{-1} and around 600 to 300 cm^{-1} as shown in Fig.3 when compared with unsonicated sample. A peak at around 1450 and 1550 cm^{-1} are particularly subdued or lost in the sonicated spectrum indicating the NH deformation thus confirming the breaking of an azo bond and formation of amine intermediates.

Scheme.1 Sonochemical degradation pathway of AR 88

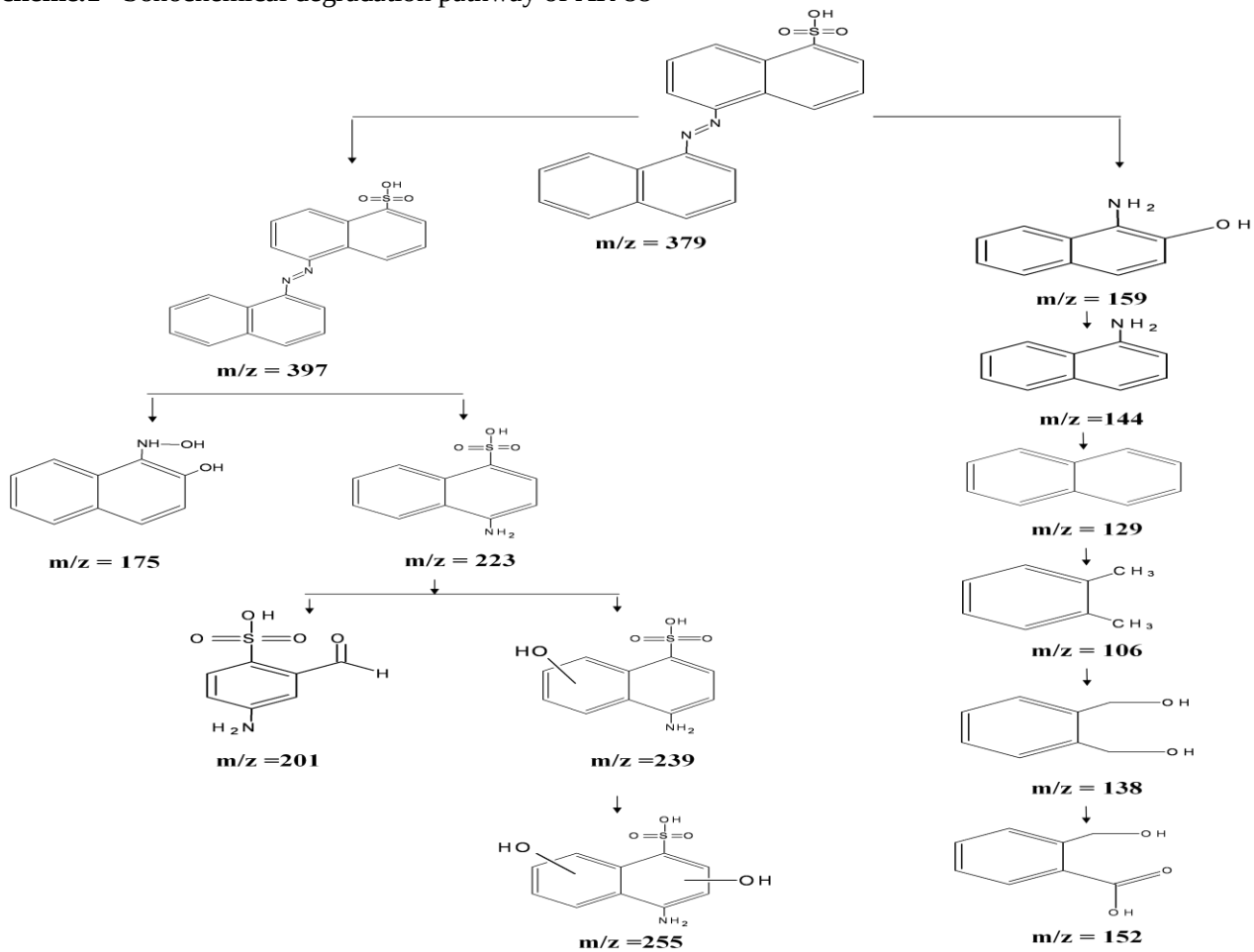

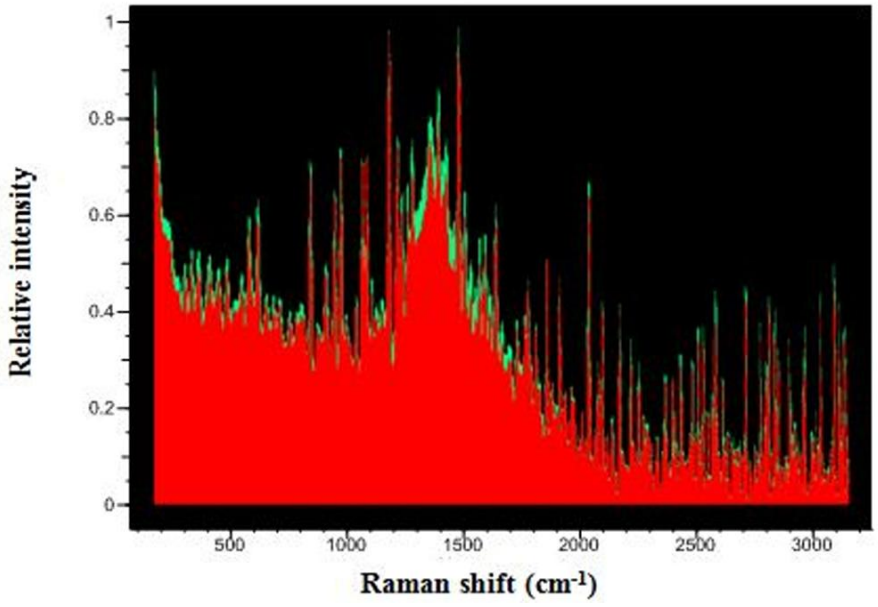

Fig. 2 Overlap density heatmap of the unsonicated and sonicated Raman spectra of Acid Red 88 dye

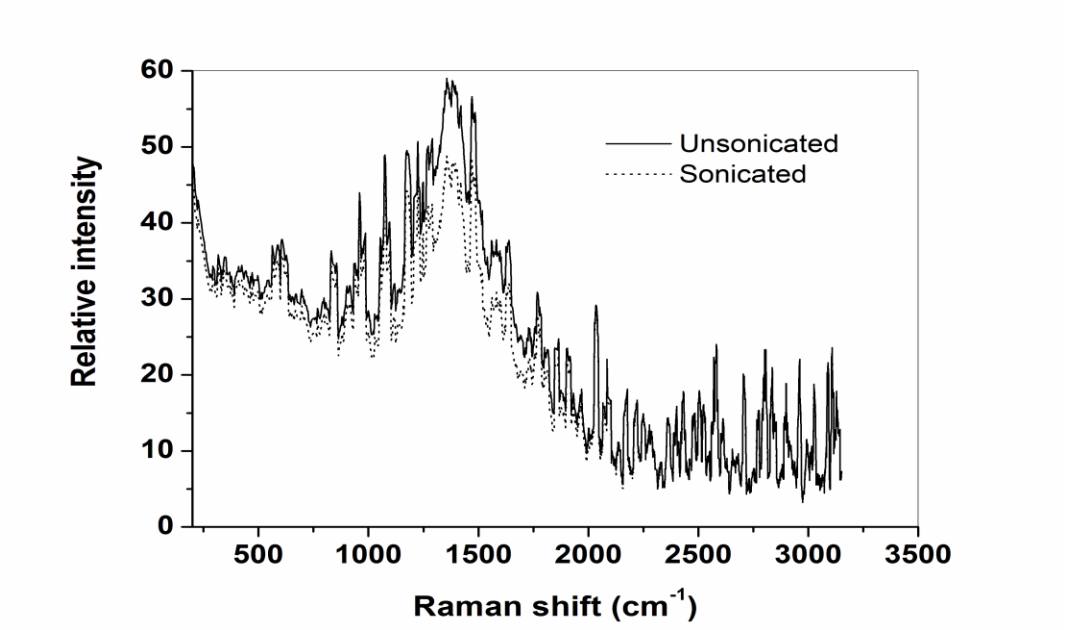

Fig.3 Raman Spectra of unsonicated and sonicated Acid Red 88 dye

APPLICATION

A detailed sono chemical degradation pathway can be suggested.

CONCLUSION

The study shows that the decolourisation of AR-88 was 97.19 % within 40 mins in the presence of ultrasound, TiO_2 and rare earths. Adsorption obeyed all the adsorption isotherms well, however, the models of Langmuir and pseudo second-order kinetics gave better explanation of the adsorption processes involved in the decolourisation of sample solution. The adsorption of AR 88 on the surface of TiO_2 was enhanced in the presence of rare earth ions due to electrostatic interaction between TiO_2, REs and dye molecule. Thus RE-TiO_2 had higher adsorption capacity (q_m) than TiO_2 alone, both in the absence and presence of ultrasound. Boyd kinetic model plot confirmed that the external masss transfer was the slowest step in the adsorption process. The formation of 4-aminonaphthalene sulphonic acid and also mono and di-hydroxylated products were identified in the sonolytic degradation path of AR 88.

ACKNOWLEDGEMENT

Authors acknowledge DAE – BRNS for the financial support, Dr. Rajesh J Tayade, CSIR, CSMCRI, Bhavnagar for the LCMS analysis and Dr. Jagvir Suhag, M/s Bio-Rad Laboratories for the Raman spectral analysis PKP is grateful to BRNS for JRF and SG to CSIR for SRF.

REFERENCES

[1] Pankaj, S. Goyal, *J. Pure & App. Ultrasonics* [In press].
[2] Pankaj, S. Goyal, Prem Kishore Patnala, *Int. J. Env. Eng. Manag*. **2012**, 3, 268-271.
[3] Pankaj, S. Goyal, R. J. Tayade, Canadian Jour. Chem. Engg. [In press].
[4] Pankaj, S. Goyal, *Mater.Sci.Forum* **2013**,734, 237 – 247. **[**In press].
[5] G.J Price, P.F Smith, *Polymer*. **1993**, 34, 4111-4117.
[6] A. Henglein, *Ultrasonics.***1987**, 25, 6-16.
[7] L.H Thompson, L.K Doraiswamy, *Ind.Eng.Chem.Res*.**1999**, 38, 1215-1249.
[8] Y.G Adewuyi, *Ind. Eng.Chem. Res*.**2005**, 40, 4681-4715.
[9] M.H Priya, G.Madras, *Ind.Eng.Chem.Res*.**2006**, 45, 913-921.
[10] M.Kubo, K.Matsuoka, A.Takahashi, N.S. Kitakawa, T.Yonemoto, *Ultrason.Sonochem*.**2005**, 12,263-269.
[11] I. Langmuir, *J.Am.Chem.Soc*.**1916**, 38, 2221 – 2295.
[12] S.Vasudevan, J. Lakshmi, R.Vanathi, *Clean-Soil Air Water*. **2010**, 38, 9-16.
[13] M.J Temkin, V.Pyzhev, *Acta.Physiochim.URSS***. 1940**, 12, 217–222.
[14] W.J Weber Jr, J.C Morris, *J.Sanit. Eng. Div. Proceed. Am. Soc. Civil Eng*.**1963**, 89, 31–59.
[15] G.E Boyd, A.W Adamson, L.S Myers Jr, *J. Am. Chem. Soc*. **1947**, 69, 2836–2848.
[16] T.Santhi, S.Manonmani,T.Smitha, *IJEST*.**2010**,2,287-295.
[17] N. K Amin, *Desalination*.**2008**, 223, 152-161.
[18] Y.S Ho, G.McKay, *Process Biochem*. **1999**, 34, 451-465.
[19] J.Madhavan, P.S.S.Kumar, S.Anandan, F.Grieser, M.Ashokkumar, *Separ. Purif. Technol*. **2010**, 74,336-341.